Quantitative Models for the Measurement of Residual Stress, Poisson Ratio and Young's Modulus Using Electrostatic Pull-in of Beams and Diaphragms

Peter M. Osterberg, Raj K. Gupta, John R. Gilbert and Stephen D. Senturia
Microsystems Technology Laboratories
Massachusetts Institute of Technology, Cambridge MA 02139, USA

ABSTRACT

This paper presents an analysis of the use of electrostatic pull-in of suspended microstructures for the measurement of material properties, and demonstrates the approach with experiments.

INTRODUCTION

Access to accurate and reliable material property data for Young's modulus, Poisson ratio and residual stress is crucial to the design of MEMS [1]. The problem is that many properties, especially residual stress, can depend not only on the specific process step used for forming a material, but also on subsequent thermal processing [2]. Even single-crystal silicon can exhibit a doping-dependent stress and stress gradient which can lead to modifications of structural stiffness and to warpage of suspended structures [3,4].

The goal of the work presented here is the design of standard "drop-in" mechanical test structures, analogous to transistor test structures used for extraction of device parameters, where the intent is to be able to measure material properties *in-situ*. There are three uses for such test structures: (1) determination of experimental engineering quantities of importance to design, such as beam stiffness, which depend on a combination of material properties and structural dimensions; (2) extraction of the primary material properties from those quantities for use in design and simulation; and (3) routine monitoring of repeatability of a complex processing sequence for MEMS devices.

If the mechanical drop-in pattern is to achieve general utility, it should be possible to perform the testing at the wafer level using ordinary wafer probe equipment and microscopes. One possible way to meet this criterion is to use electrostatic deflection and pull-in of microstructures, detected either electrically or optically. Najafi and Suzuki [5] have already proposed this approach and have presented results on various microelectronic materials. Their work, however, was based on simple analytical models of beam behavior and electrostatic applied loads. We are now revisiting this subject using more intensive 2-D and 3-D numerical modeling tools developed for the MIT MEMCAD system [6-8].

At MEMS 94, we reported a hierarchy of models for electrostatic pull-in [8]. In this work, we significantly extend those models, both by the development of closed-form expressions for pull-in voltage of cantilevers, fixed-fixed beams, and clamped circular diaphragms, and by the inclusion of a first-order correction for electrostatic fringing fields (following a suggestion of Crary [9]). The closed-form expressions permit a succinct discussion of the benefits and limitations of electrostatic pull-in as a method for material property extraction. The method is then illustrated using measurements on suspended fixed-fixed beams processed in wafer-bonded single-crystal-silicon [10], and on suspended fixed-fixed beams of aluminum-coated silicon nitride [1 1].

MODELS OF ELECTROSTATIC PULL-IN

Previously Reported Models. As presented in [8], we use a hierarchy of models to explore the pull-in behavior of cantilevers, fixed-fixed beams, and clamped circular diaphragms insulated from and suspended above a ground plane by a gap g_o. These structures are illustrated in Figure 1. The simplest model of electrostatic actuation of these structures is a 1-D parallel-plate capacitor with one fixed plate and one plate suspended from an ideal linear spring as shown in Figure 2. If we neglect fringing fields, we can write the force balance for this system as

$$K(g_o - g) = \frac{\varepsilon_o V^2 A}{2g^2} \quad (1)$$

where g is the gap between the structure and the ground plane, g_o is the initial gap, K is a lumped mechanical spring constant for the structure, V is the applied voltage, ε_o is the permittivity, and A is the area of the capacitor plate. This system has a well-known pull-in instability, as illustrated in Figure 3, which plots the gap normalized to its initial value versus the applied voltage normalized to the pull-in voltage, V_{PI}. For voltages less than V_{PI}, the structure is stable. As V approaches V_{PI} and g approaches $2g_o/3$, the plate position becomes unstable, and collapses to the ground plane. The expression for pull-in voltage is

$$V_{PI} = \sqrt{\frac{8Kg_o^3}{27\varepsilon_o A}} \quad (2)$$

The importance of this 1-D model is that it provides a closed-form expression for the pull-in voltage in terms of parameters such as a "spring constant", "capacitor gap", and "capacitor area". Note that the spring constant K, which typically includes both structural dimensions and material properties, appears in a product with g_o^3. This means that a measurement of V_{PI} alone cannot separate the material properties from the geometric quantities, even if the area A is systematically changed. We will discuss this point in greater detail later.

As demonstrated in [8], when we attempt to determine K from the small-deflection beam or diaphragm differential equations by applying a uniform pressure load and finding the maximum deflection, we find that the pull-in voltage predicted by Eq. 2 is significantly in error. The primary reason is that the rigid-parallel plate capacitor is a bad model for a bending beam or diaphragm. Instead, we used the beam and diaphragm differential equations (in effect, a 2-D structural model) with a position dependent electrostatic load. The load was derived from the expression for the force on an incremental parallel-plate capacitor whose value varies inversely with the position-dependent gap, g. A similar force model has been previously used by Artz and Cathey [12] in conjunction with finite-element simulations. As an illustration, the

0-9640024-0-X/hh1994/$20©1994TRF
DOI 10.31438/trf.hh1994.42

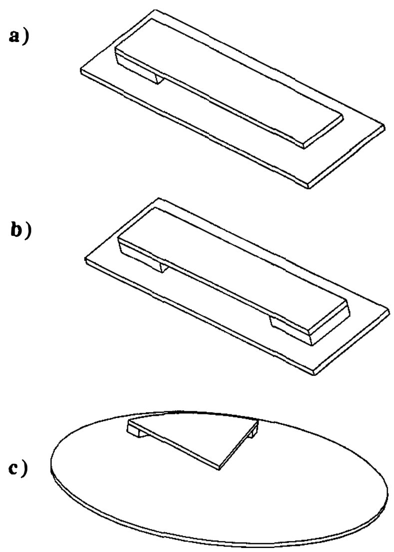

Figure 1.Test structures: (a) cantilever beam, (b) fixed-fixed beam, (c) clamped circular diaphragm (cut-away view).

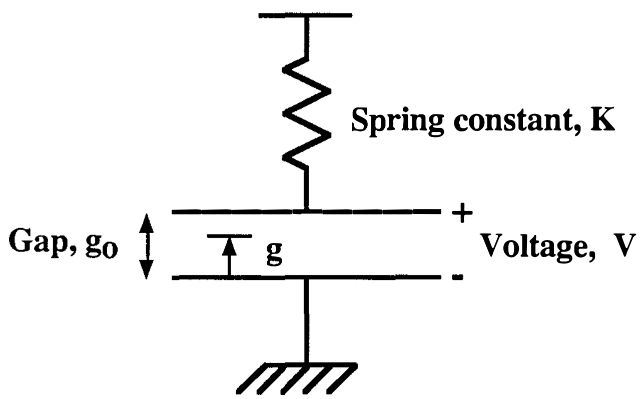

Figure 2. 1-D lumped parallel-plate capacitor model.

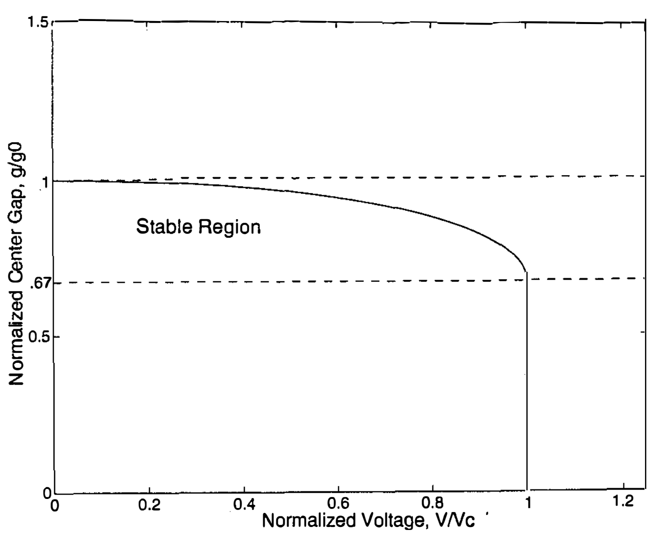

Figure 3. Normalized plot of the gap vs voltage for the 1-D lumped model. Stability requires a normalized gap, g/g_0, greater than 2/3.

differential equation for a fixed-fixed beam under this assumption becomes

$$EI\frac{d^4g}{dx^4} - T\frac{d^2g}{dx^2} = -\frac{\varepsilon_0 V^2}{2g^2}\left(1+0.65\frac{g}{w}\right) \qquad (3)$$

where E is Young's modulus, $I=(1/12)wt^3$, $T=\sigma_0(1-\nu)wt$, w is beam width, t is beam thickness, σ_0 is the biaxial residual stress presumed present before the beam shape was etched, ν is the Poisson ratio, and the factor in parentheses on the right-hand side is a new fringing-field correction, explained below.

While it was acceptable in [8] to neglect fringing fields when studying clamped circular diaphragms, it is more important to examine fringing when analyzing the behavior of beams, since the fringing fields occur in a region which is changing shape due to deflection. The origin of the correction term in Eq. 3 is an analytic expression for the capacitance of a zero-thickness stripline over a ground plane, as obtained by Morganthaler [13]. Morganthaler's capacitance formula was then differentiated with respect to gap to give the fringing-field enhancement of the electrostatic force for a parallel plate capacitor. The result is the right-hand side of Eq. 3. This correction does not take into account the finite thickness of the beam, but preliminary studies on two-dimensional electrostatic geometries of beam structures show that a correction to account for thickness will not increase capacitance values more than a few percent for $g/w < 0.1$. Nevertheless, the effect of finite thickness may slightly modify the calculated pull-in voltages reported here for beams and cantilevers; study of these details is continuing.

Numerical finite-difference solution of Eq. 3 (and of the corresponding equations for cantilevers and clamped circular diaphragms) was performed using Newton's method implemented in MATLAB [14]. In [8] it was shown that the gap vs. voltage and the value of the pull-in voltage from the 2-D numerical model for a clamped circular diaphragm agreed well both with a full 3-D self-consistent electromechanical simulation and with experimental data on a suspended diaphragm consisting of a tensioned polymer membrane with a thin aluminum coating. We also expect the 2-D models with fringing correction to be reasonably accurate for cantilevers and beams over ground planes when the aspect ratio (gap relative to beam width) is small, and when the gap is small enough so that the pull-in instability is reached before the beam bending enters the large-deflection regime.

Closed-form models for mechanical property extraction. In order to use the 2-D simulations for mechanical property extraction, we have captured the results of numerical analysis into closed-form expressions which make explicit the dependence of key model parameters on material properties and structural dimensions. In previous work, we have used this approach to establish a quantitative basis for the load-deflection method for extracting residual stress and biaxial modulus, $E/(1-\nu)$, of tensile suspended membranes [15,16]. The approach in the present work is to find the analytical form of the "effective spring constant" from a solution of the beam or diaphragm equation with a uniform distributed load, and replace the numerical constants in the solution by fitting parameters which, if successful, can capture the corrections needed to allow for the fact that when the structure deflects, the load is no longer uniform. The results of the 2-D numerical simulations are then fitted to the analytical expression, leading to a semi-numerical closed-form expression for pull-in voltage as a function of both material properties and structural dimensions.

TABLE I. Closed-form expressions for pull-in voltage of suspended structures defined in terms of the numerical constants in TABLE II and parameters in TABLE III. The index n equals 1 for cantilevers, 2 for fixed-fixed beams, and 3 for clamped circular diaphragms. L is either length (for cantilevers and beams) or radius (for diaphragms). In the stress-dominated limit, $k_n L \gg 1$, and in the bending dominated limit, $k_n L \ll 1$.

	General	Stress Dominated	Bending Dominated
V_{PI}	$\sqrt{\dfrac{\gamma_{1n} S_n}{\varepsilon_o L^2 D_n(\gamma_{2n}, k_n, L)\left[1+\gamma_{3n}\dfrac{g_o}{w}\right]}}$	$\sqrt{\dfrac{\gamma_{1n} S_n}{\varepsilon_o L^2\left[1+\gamma_{3n}\dfrac{g_o}{w}\right]}}$	$\sqrt{\dfrac{4\gamma_{1n} B_n}{e_o L^4 \gamma_{2n}^2\left(1+\gamma_{3n}\dfrac{g_o}{w}\right)}}$

where $$D_n = 1 + \frac{2\{1-\cosh(\gamma_{2n} k_n L/2)\}}{(\gamma_{2n} k_n L/2)\sinh(\gamma_{2n} k_n L/2)}$$ and $$k_n = \sqrt{\frac{12 S_n}{B_n}}$$

TABLE II: Numerical constants for the closed form expressions of TABLE I.

Numerical Constants	n = 1	n = 2	n = 3
γ_{1n}	0.28	2.79	1.55
γ_{2n}	N/A	0.97	1.65
γ_{3n}	0.42	0.42	0

TABLE III: Stress and Bending Parameters for the closed-form expressions of TABLE I.

	n = 1	n = 2	n = 3
S_n	0	$\sigma_o(1-\nu)tg_o^3$	$\sigma_o t g_o^3$
B_n	$Et^3 g_o^3$	$Et^3 g_o^3$	$\dfrac{Et^3 g_o^3}{(1-\nu^2)}$

Tables I-III contain the closed-form models. Table I shows the general form of the pull-in voltage, where the index n=1 refers to cantilevers, n=2 to fixed-fixed beams, and n=3 to circular diaphragms. The analytical form depends on two parameters, S_n and B_n, which combine geometric factors with either stress or modulus, respectively (see Table III). The ratio, S_n/B_n, appears in the factor k_n, which is a measure of the relative importance of stress versus bending. The stress-dominated limit is $k_n L \gg 1$ and the bending dominated limit is $k_n L \ll 1$. Asymptotic forms for these two limits are also shown in Table I.

For each structure type, several thousand self-consistent calculations of pull-in voltage versus were carried out using the 2-D model on MATLAB, systematically varying S_n and B_n. The results of these simulations for each structural type ("the virtual data") were then fit to the form in Table I using three parameters γ_{1n}, γ_{2n}, and γ_{3n} (except that the fringing term is not used for circular diaphragms). The resulting values are shown in Table II. Figure 4 illustrates a typical comparison between the 2-D numerical simulations and the fit from the closed-form model. The typical agreement of V_{PI} is within 10 mV or better.

EXTRACTION OF MATERIAL PROPERTIES

Strategy. In a typical MEMS process, structural thicknesses and gap heights are fixed. Structural widths and lengths can be readily varied by mask design. A useful strategy, therefore, is to measure V_{PI} versus beam length (or diaphragm radius). In order to extract material properties, it is first necessary to fit the experimental data to the form of the expressions in Table I by determining numerical values for S_n and B_n. Then, using known values of thickness and initial gap, one can extract material properties.

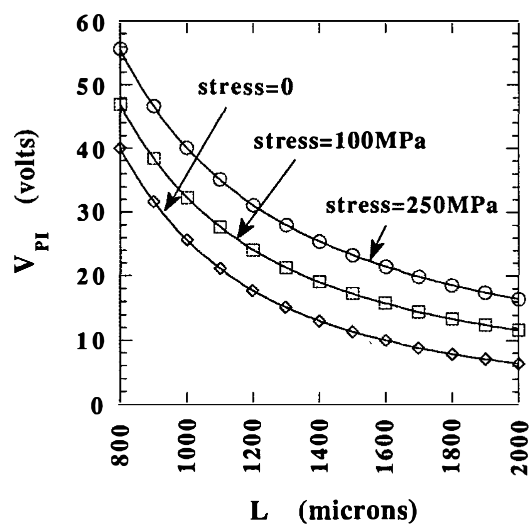

Figure 4. Comparison of closed-form model (solid line) to 2-D MATLAB simulated pull-in (points) for three fixed-fixed beams with varied stress (E=169 GPa, ν=0.3, width= 50μm, thickness=14.4μm and g_0=1μm in each case). Agreement is typically within 10 mV.

If only cantilevers are used, then only B_1 can be determined (S_1 is always zero). The other two structures in general will yield values for both S_n and B_n, although for extreme values of k, one of these may be very noisy (see below). If S_2 and S_3 can be found, then their ratio yields ($1-\nu$) without any additional depen-dence on geometric factors. Similarly, B_2/B_3 equals ($1-\nu^2$). However, extraction of either E or σ_o requires independent deter-mination of t and g_o. Further, since S_n and B_n depend on g_o^3, errors in g_o appear amplified by a factor of 3 in the extraction of σ_o from S_n or E from B_n. Errors in t appear similarly amplified in the extraction of E from B_n. We now examine how this works in practice.

Experimental Methods. We obtained from Hsu [10] a wafer containing silicon fixed-fixed beams fabricated in a dielectrically isolated wafer-bonding process. The beams are 14.4 ± 0.2 μm thick, 50 μm wide and are suspended above the ground plane by an initial gap of 1.015 ± 0.01 μm. Beam lengths varied between 900 μm and 1500 μm, using drawn mask dimensions for length.

To measure pull-in, a slowly ramped voltage was applied between the beam and the substrate, and the current was recorded. Pull-in was indicated by the appearance of contact current. Figure 5 shows an example output from a typical pull-in experiment using this technique. Pull-in voltage could be determined in this fashion to within better than 0.1 V. A total of nine die, each containing five beams of different lengths, were tested.

Experimental Results. Figure 6 shows a plot of pull-in voltage versus beam length for a series of five beams from one die located near the center of the wafer. The solid curve is the fit to the closed-form model using the non-linear least-squares algorithm in Kaleidagraph [17]. The result indicated a very small value for S_2 with a large relative error ($S_2 = 2 \pm 1 \times 10^{-20}$ Pa-m^4) and a reltively accurate value for B_2 ($5.4 \pm 0.1 \times 10^{-22}$ Pa-m^6). The fact that S_2 is not statistically well defined suggests that the behavior is bending dominated. Therefore, as a test, we assumed $S_2=0$ and did an independent fit to the asymptotic form of the bending dominated expression in Table I. In that case only the factor B_2 enters, and we obtained $5.3 \pm 0.1 \times 10^{-22}$ Pa-m^6. The good agreement between the two fitting procedures indicates that numerical artifacts are not dominating the results, and that the stress in the silicon is small.

Extraction of Young's modulus and residual stress from this one die depends directly on the accuracy with which the geometric parameters are known. Using the stated experimental uncertainties on t and g_o, we calculate a range for Young's modulus: E=173 ± 13 GPa and an upper bound for residual stress: $\sigma_o(1-\nu) < 100$ KPa (estimated from the tolerance of the fitting routine). On other die, we found larger tolerances corresponding to a bound of $\sigma_o(1-\nu) < 10$ MPa, but we never obtained a well-defined non-zero value for S_2. The value of modulus agrees well with the known Young's modulus of 169 GPa for a [110] directed beam in a <100> single crystal plane [18], but has a much larger uncertainty than the B_2 value because of the amplified uncertainties in t and g_o.

In examining die-to-die variation, we find a range of B_2 between 4.1 and 5.4×10^{-22} Pa-m^6 for die near the center of the wafer, and much larger variation near the edge of the wafer. The variations are substantially larger than the precision with which B_2 can be determined for each die, and therefore suggest that there are variations in structural geometry from die to die. This is being examined further.

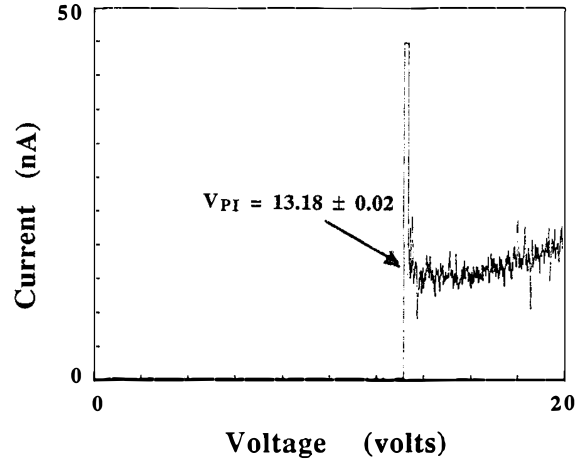

Figure 5. Current-voltage characteristic of a dielectrically isolated fixed-fixed silicon beam (length=1500μm, width=50μm, thickness=14.4μm, g_o=1μm). Pull-in is indicated by the abrupt jump in current.

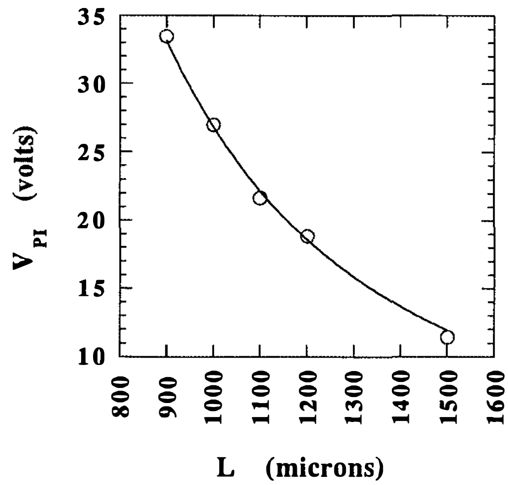

Figure 6. Experimental pull-in data vs beam length for a series of five beams from one die. Solid line is the fit to the closed-form model which yields:$B_2 = 5.4 \pm 0.1 \times 10^{-22}$ Pa-m^6 and $S_2 < 1 \times 10^{-19}$ Pa-m^4.

A second set of samples was obtained from Bloom at Stanford [11]. The structures were fixed-fixed beams of LPCVD silicon nitride (nominally 1325 Å thick and 1.25 μm wide) coated with aluminum (200 Å thick), suspended 1325 Å above a ground plane. Beam lengths ranging from 28 μm to 40 μm were tested. Pull-in of these structures was observed visually by microscope. In contrast with the silicon beams, which were bending dominated, a fit to the V_{PI} vs L data yielded good precision on S_2 ($6.0 \pm 0.1 \times 10^{-20}$ Pa-m^4), and a small value for B_2 ($5.0 \pm 1.0 \times 10^{-29}$ Pa-m^6). Their ratio indicates that this case is tension dominated. Because of substantial uncertainties in geometry for these devices, including some underetching of the supports at the ends and ambiguity on how to define the value of g_o in this dual-dielectric structure, we did not attempt a quantitative study of residual stress.

DISCUSSION AND CONCLUSIONS

We have presented closed-form models for the electrostatic pull-in behavior of suspended cantilevers, fixed-fixed beams, and clamped circular diaphragms. These models are based on 2-D numerical simulation of beam deflection, including a first-order fringing-field correction. The expressions are directly usable by designers for prediction of pull-in. We have further shown that experimental data on such structures can be used to extract parameters (S_n and B_n) which depend on combinations of mechanical properties and structural geometry. These parameters are very useful indicators of structural stiffness, and show directly whether the behavior is stress-dominated or bending dominated. They can also serve to monitor the repeatability of a fabrication process. However, because these quantities depend on thickness and initial gap to a higher power than Young's modulus or residual stress, errors in geometric parameters generate relatively larger errors in the extracted mechanical properties. Thus, it is clear that this method puts a stringent demand on the metrology of structural dimensions. An important next step is the examination of *in-situ* methods for monitoring critical dimensions, so that the precision of the extracted mechanical properties can be improved.

ACKNOWLEDGMENTS

This work was supported in part by the Semiconductor Research Corporation (Contract 93-SC-309) and by ARPA (Contract J-FBI-92-196). The authors wish to thank Charles Hsu and Prof. Martin Schmidt of MIT and Dr. David Bloom and Dr. Raj Apte of Stanford for providing devices used in this work, and for helpful technical discussions. Measurements were made using Prof. Schmidt's test station. The authors also wish to thank Dr. Selden Crary of the University of Michigan for his suggestion of an approach to the problem of fringing-field corrections.

REFERENCES

[1] S. D. Senturia, "Microfabricated structures for the measurement of mechanical properties and adhesion," *Proc. Transducers '87*, Tokyo, Japan, June 1987, pp. 11-16.

[2] S. D. Senturia, "Mechanical properties of microsensor materials: How to deal with the process dependencies?" *Mat. Res. Soc. Symp. Series*, **239**, 3-11 (1992).

[3] W.-H. Chu and M. Mehregany, "A study of residual stress distribution through the thickness of p+ silicon films," *IEEE Trans. Elec. Dev.*, **40**, 1245-1250 (1993).

[4] F. Maseeh and S. D. Senturia, "Plastic deformation of highly doped silicon," *Sensors and Actuators*, A**21**-A**23**, 861-865 (1990).

[5] K. Najafi and K. Suzuki, "A Novel Technique and Structure for the Measurement of Intrinsic Stress and Young's Modulus of Thin Films," *Proc. MEMS 89*, Salt Lake City, Feb. 1989, pp. 96-97.

[6] J. R. Gilbert, P. Osterberg, R. Harris, D. Ouma, A. Pfajfer, J. White, and S.D. Senturia, "Implementation of a MEMCAD System for Electrostatic and Mechanical Analysis of Complex Structures from Mask Descriptions", *Proc. MEMS 93*, Fort Lauderdale, Florida, Feb. 1993, pp. 207-212.

[7] X. Cai, H. Yie, P. Osterberg, J. Gilbert, S. D. Senturia, and J. White, "A Relaxation/Multipole-Accelerated Scheme for Self-Consistent Electromechanical Analysis of Complex 3-D Microelectromechanical Structures," *Intl. Conf. Computer Aided Design*, Santa Clara, CA, Nov. 1993, pp. 270-274.

[8] P. Osterberg, H. Yie, X. Cai, J. White and S. Senturia, "Self-Consistent Simulation and Modeling of Electrostatically Deformed Diaphragms", *Proc. MEMS 94*, Oiso, Japan, Jan. 1994, pp. 28-32.

[9] Dr. Selden Crary, private communication.

[10] C. H. Hsu and M. A. Schmidt, "Micromachined Structures Fabricated Using Wafer-Bonded Sealed Cavity Process", *1994 Solid-State Sensor and Actuator Workshop*, Hilton Head, SC, June 1994 (this volume).

[11] O. Solgaard, F. S. A. Sandejas, and D. M. Bloom, "Deformable grating optical modulator," *Optics Letters*, **17**, 688-690 (1992).

[12] B. E. Artz and L. W. Cathey, "A Finite Element Method for Determining Structural Displacements Resulting from Electrostatic Forces", *IEEE Solid-State Sensor and Actuator Workshop*, Hilton Head, SC, June 1992, pp. 190-193.

[13] F. R. Morgenthaler, "Theoretical Studies of Microstrip Antennas, Vol. 1: General Design Techniques and Analyses of Single and Coupled Elements", U. S. Dept. of Transportation, Federal Aviation Administration Report No. FAA-EM-79-11, I, September 1979.

[14] Matlab is a commercial product from The Mathworks Inc, Natick, MA, USA. Matlab scripts for the solution of the 2-D case for cantilevers, fixed-fixed beams and circular diaphragms, including the fringing-field correction, are available from the authors.

[15] P. Lin, *et. al.*, "The in-situ measurement of biaxial modulus and residual stress of multi-layer polymeric thin films", *Mat. Res. Soc. Symp. Series*, **188**, 41-46 (1990).

[16] Jeffrey Y. Pan, PhD Thesis, Department of Electrical Engineering and Computer Science, Massachusetts Institute of Technology, September 1991; also J. Y. Pan and S. D. Senturia, "Suspended-membrane methods for determining the effects of humidity on the mechanical properties of thin polymer films," *Soc. Plast. Eng. 49th Annual Tech. Conf., (ANTEC '91)*, Montreal, Canada, April 1991.

[17] Kaleidagraph Version 2.1.3, Adelbeck Software.

[18] W. A. Brantley, "Calculated elastic constants for stress problems associated with semiconductor devices," *J. Appl. Phys.*, **44**, 534-535 (1973).